Journal of Power Sources 227 (2013) 177–184

Contents lists available at SciVerse ScienceDirect

Journal of Power Sources

journal homepage: www.elsevier.com/locate/jpowsour

Improvement in self-discharge of Zn anode by applying surface modification for Zn–air batteries with high energy density

Sang-Min Lee [a,*], Yeon-Joo Kim [a], Seung-Wook Eom [a], Nam-Soon Choi [b], Ki-Won Kim [c], Sung-Baek Cho [d]

[a] Battery Research Center, Korea Electrotechnology Research Institute, Changwon 641-120, Republic of Korea
[b] Interdisciplinary School of Green Energy, Ulsan National Institute of Science and Technology, Ulsan 689-798, Republic of Korea
[c] School of Advanced Material Engineering, Gyeongsang National University, 900 Gajwa-dong, Jinju 660–701, Republic of Korea
[d] Agency for Defense Development, Bugyuseong daero 488, Daejeon 305-152, Republic of Korea

HIGHLIGHTS

- Self-discharge of Zn-air battery was remarkably suppressed by surface modification of Zn anode.
- Al_2O_3 coating is very effect on controlling the hydrogen evolution reaction on Zn anode.
- Overpotential for hydrogen evolution was measured by potentio-dynamic polarization analysis.
- A surface-treated Zn electrode shows improved performances of energy density and cycle life.

ARTICLE INFO

Article history:
Received 6 September 2012
Received in revised form
15 November 2012
Accepted 16 November 2012
Available online 23 November 2012

Keywords:
Self-discharge
Overpotential
Hydrogen evolution
Surface modification

ABSTRACT

The self-discharge of Zn anode material is identified as a main factor that can limit the energy density of alkaline Zn–air batteries. Al_2O_3 has most positive effect on controlling the hydrogen evolution reaction accompanied by corroding Zn anode among various additives. The overpotential for hydrogen evolution is measured by potentio-dynamic polarization analysis. Al-oxide with high overpotential for hydrogen evolution reaction is uniformly coated on the surface of Zn powders via chemical solution process. The morphology and composition of the surface-treated and pristine Zn powders are characterized by SEM, EDS, XRD and XPS analyses. Aluminum is distributed homogeneously over the surface of modified Zn powders, indicating uniform coating of Al-oxide, and O1s and Al2*p* spectra further identified surface coating layer to be the Al-oxide. The Al-oxide coating layer can prevent Zn from exposing to the KOH electrolyte, resulting in minimizing the side reactions within batteries. The 0.25 wt.% aluminum oxide coated Zn anode material provides discharging time of more than 10 h, while the pristine Zn anode delivers only 7 h at 25 mA cm^{-2}. Consequently, a surface-treated Zn electrode can reduce self-discharge which is induced by side reaction such as H_2 evolution, resulting in increasing discharge capacity.

© 2012 Elsevier B.V. All rights reserved.

1. Introduction

Zn–air batteries, because of their high specific energy, environmental compatibility and low-cost materials, have long been considered to be potentially attractive as power sources for mobile application including electric vehicles [1–6]. In particular, Zn–air battery possesses the highest specific energy density compared with other Zn-based alkaline batteries. This is mainly due to unlimited and free supply of oxygen from ambient air which is not incorporated within the cell. The Zn–air cell has a theoretical specific energy of 1085 $Whkg^{-1}$, based on the molecular weight of ZnO (658 $Ahkg^{-1}$) and the theoretical cell voltage 1.65 V [7]. The overall cell discharge reactions can be summarized as follows [8].

At the positive (cathode) electrode:

$$O_2 + 2H_2O + 4e^- \rightarrow 4OH^-, \quad E^0 = 0.40\ V\ (\text{vs. SHE})$$

At the negative (anode) electrode:

$$Zn^{2+} + 2OH^- \rightarrow ZnO + H_2O + 2e^-, \quad E^0 = 1.25\ V\ (\text{vs. SHE})$$

Overall cell reaction:

$$2Zn + O_2 \rightarrow 2ZnO, \quad E^0 = 1.65\ V$$

The main disadvantage of both primary and secondary Zn–air batteries is their early degradation due to corrosion of the Zn

* Corresponding author. Tel.: +82 55 280 1663; fax: +82 55 280 1590.
E-mail address: sangma@keri.re.kr (S.-M. Lee).

0378-7753/$ – see front matter © 2012 Elsevier B.V. All rights reserved.
http://dx.doi.org/10.1016/j.jpowsour.2012.11.046

anode material and clogging in air cathode induced by carbonation of the KOH electrolyte [9]. Obviously, Zn has a more negative reduction potential than hydrogen, which spontaneously leads to evolve hydrogen gas on Zn particle surface [10]. The hydrogen evolution reaction (HER) in an alkaline battery while in storage is given by reaction below [8,11].

$$Zn + 2H_2O \rightarrow Zn(OH)_2 + H_2\uparrow$$

Therefore, the surface of Zn is gradually oxidized to the sub-surface while a battery is in storage at a state of partial discharge. This disadvantage needs to be solved for Zn secondary batteries to be commercialized successfully. Many attempts have been made to suppress hydrogen gas evolution. Mercury has been found to be the most effective additive for suppressing hydrogen evolution reaction, but is prohibited from use due to environmental concerns [12,13]. As alternative, other additives such as metal, metal compound have also been proposed [14–17]. Bismuth and In also increase the hydrogen overpotential of the Zn anode, are considered as environmentally friendly, and have replaced Hg and Pb in Zn alloy battery powders [14,15].

Lee et al. [15] reported that alloying Zn metal with nickel and indium is effective in shifting to more negative potentials for hydrogen evolution. Zhang et al. [18] suggested that introducing metallic bismuth to a pasted Zn electrode improved the discharge performance because of the formation of an electronic conductive material. The alloy design to suppress Zn corrosion, however, has been limited by intrinsic material properties of Zn, for example, too narrow solid-solution region in Zn element to alloy with various foreign elements and comparatively low melting temperature of Zn (m.p. 419 °C). Therefore, the improvement of Zn corrosion by alloying is supposed to be not so much due to limited choice of some elements alloyed with Zn.

In this paper, the effects of surface coverage on Zn corrosion by metallic oxide coating, instead of alloy design, will be investigated. To get comparable corrosion resistance without adding mercury into Zn, it has been tried to apply metallic oxide additives as an alternative to mercury to suppress Zn corrosion. Furthermore, to maximize the effect of additives on hydrogen overpotential, the surface of Zn particles was modified with nano-sized metallic oxide particles via chemical solution process. In addition, the effects of the surface modified Zn electrodes on battery performance will be studied with respect to electrochemical and phenomenological phenomena to clarify its effect on suppressing the hydrogen evolution reaction.

2. Experimental details

2.1. Synthesis of Zn powders coated with metallic oxide

The pure metallic Zn powder (purity>99.99%, D_{50} = 52 μm, Aldrich) as reference material has been chosen to compare the electrochemical characteristics with modified Zn anode. Additionally, the metallic oxides have been considered as a coating material for surface modification through chemical solution synthesis. Thus, in this work, the metallic oxides such as Al_2O_3, Bi_2O_3, and In_2O_3 powders as various additives were applied for Zn-based anode. It has been also reported that some of metallic oxides had an influence on shifting hydrogen evolution potential of Zn anode [19]. Therefore, it is needed to examine the effect of metallic oxides on the corrosion behavior of Zn anode to select the most preferable additive prior to surface modification.

Among these additives, it has been found that the Al_2O_3 showed the most favorable performances to Zn anodes. It will be discussed in detail in Section 3. The Zn powder coated with 0.25 wt% of Al_2O_3 was synthesized by sol–gel process. The Al_2O_3 coating was synthesized according to a following procedure from appropriate amount of Al-isopropoxide ($Al(OC_3H_7)_3$ > 98%, Aldrich) powder dispersion in hydrous ethanol (95%) with constant stirring at 298 K for 5 h to get nearly transparent sol product. Then, the Zn powders were added into the above dispersion and ultrasonificated for 1 h. A subsequent slow evaporation of the ethanol at 80 °C resulted in getting dry mass of Al-isopropoxide coated Zn powders. It was then heated up to 400 °C at a heating rate of 5 °C min^{-1} and held at 400 °C for 3 h. The heat treatment temperature (400 °C) was chosen lower than melting point (419.5 °C) of pure Zn (>99.9%). The cooling rate of the furnace was also 2 °C min^{-1}. To assist in the understanding crystallization behavior of the gel coating on Zn surface upon heating, we conducted thermogravimetric (TG) and differential scanning calorimetry (DSC) analyses on Al-isopropoxide powders following the same drying and heating schedule.

2.2. Preparation of Zn-based gel anode

It is well understood that the high surface area of battery electrode is favorable to kinetics related performances of battery. Likewise, in the Zn–air system, the most practical method of improving the performance of the Zn anode is to increase the reaction surface area of the Zn powder so that Zn can react with the alkaline electrolyte more efficiently. Therefore, a recent approach of porous electrode with various shaped Zn powders, not just planar Zn electrodes, has also received attention [20].

The pasted Zn electrode were prepared from an aqueous slurry containing Zn-based powder (or Aluminum oxide coated Zn powder), traces of additives (2 wt.% of Al_2O_3, Bi_2O_3, In_2O_3) to suppress hydrogen evolution, and PAA (Poly acrylic acid, Mw = 1,250,000 Aldrich) as a gelling agent. The gelling agent has immobilizing ability, which is required to store aqueous alkaline solution, leading to minimize the volume of the cell. Upon mixture with solution, the gel expands into a loosely bound gel film and thus reduces the amount of electrolyte that is required to occupy a particular cell volume [21–23]. The electrolyte composition was fixed to be 9 M KOH saturated aqueous solution to minimize hydrogen evolution reaction [24].

2.3. Material characterization

The crystal structure of coated layer by surface modification was identified by the X-ray diffraction method (Siemens D5000). Diffraction patterns were acquired with nickel-filtered Cu Kα radiation between scattering angles of 15° and 80° in increments of 4°. The morphology and size of the Zn-based particles were examined by scanning electron microscopy (SEM, Hitachi model S-4800). The composition of coating layer was confirmed with energy dispersive X-ray spectrometry (EDS, Hitachi model S-4800). Furthermore, the chemical states of constituting elements in coating layer (aluminum, and oxygen) were analyzed by X-ray photoelectron spectroscopy instrument (XPS, VG Scientific ESCALAB 250) with monochromatic Al Kα radiation of 1486.6 eV.

2.4. Measurement of Zn corrosion rate in alkaline electrolyte

Based on reaction $Zn + 2H_2O \rightarrow Zn(OH)_2 + H_2\uparrow$ [8,11], the corrosion rate could be derived by volumetric measurement of the hydrogen evolution as a function of reaction time with alkaline solution. The gas collecting apparatus consisted of a glass vial with airtight cap and a cylindrical graduated Teflon tube fed with paraffin, as described in Ref. [25]. The volumetric measurement was performed at elevated temperature of 60 °C to accelerate hydrogen

evolution rate. The pure Zn powders of 0.74 g excluding 2 wt.% additives were packed in a 1.6 cm^2 separator bag, which was placed into a glass vial filled with 9 M KOH. The vial was sealed airtight and connected to a capillary tube containing 10 ml of paraffin. Levels of paraffin were monitored during 5 h. As Zn corrosion accompanies with subsequent hydrogen evolution, the paraffin level can be interpreted as a function of the corrosion rate.

2.5. Potentio-dynamic polarization experiment

To investigate the polarization behavior of Zn anode modified with different additives, we have assembled 3-electrodes cell including Zn-based electrode served as a working electrode, Hg/HgO served as a reference electrode, and Pt wire served as a counter electrode [26]. The potentio-dynamic polarization measurements were performed employing a computer-controlled Solartron 1287 electrochemical interface. All the experiments were carried out at room temperature. We scanned from −200 mV to 400 mV at a scan rate of 20 mV min^{-1}, referring to open circuit potential between Zn working electrode and Pt counter electrode to compare the polarization degree on hydrogen evolution reaction of different Zn anodes. In case of calculating corrosion current, which corresponds to hydrogen evolution rate at equilibrium state, the surface area refers to the apparent surface area of each electrode.

2.6. Fabrication of Zn–air unit cell and its charge-discharge test

Fig. 1 shows the assembly of the alkaline Zn-air cell designed in this work. The cell consists of rectangular shaped Teflon and stainless steel (SUS316) casing containers, 6.5 cm in length and 5 cm in width, in which we assembled the components of the cell in the order: a Zn-based gel as an anode (2.07 g of Zn powder, 2.5 cm × 2 cm × 0.2 cm), microporous polypropylene membrane (a Celgard 3501 separator, 5 cm × 3 cm × 0.01 cm) being soaked in a 9 M (37 wt.%) KOH solution, and a commercialized carbon-based air cathode (6 cm × 2 cm × 0.1 cm) that was sufficiently porous and permeable to air. Furthermore, an SUS316 plate, which had a volume of 3.25 cm^3 (6.5 cm × 5 cm × 0.1 cm) with 38 small holes (diameter 0.1 cm), was placed next to the cathode to allow air passing to be limited. To avoid self-discharge of Zn anode in contact with air, the SUS plate was kept closed until the cell was ready to discharge. The alkaline Zn–air cell was charged and discharged at an applied current of 25 mA cm^{-2} and a discharge cut-off voltage of 0.2 V using multi-channel battery tester (Toyo system) at 25 °C.

3. Results and discussion

3.1. Corrosion behavior of Zn anode with various additives

To select proper additives for surface modification, we added metallic oxides as candidate additives to pure Zn gel anode and then examined the corrosion rate during exposing to air atmosphere. Fig. 2 shows the volumetric amount of hydrogen spontaneously evolved from Zn gel with various additives immersed in 9 M KOH during 5 h at elevated temperature of 60 °C. The volumetric measurement was intentionally performed at elevated temperature to highlight each additive's effect on hydrogen evolution reaction. The pure Zn gel anode has highest H_2 evolution rate, comparing with other modified Zn gel anodes with additives. It is obvious that the metallic oxide, in itself, plays a role in retarding the spontaneous corrosion reaction ($Zn + 2H2O \rightarrow Zn(OH)_2 + H_2\uparrow$) of pure Zn gel anode immersed in saturated alkaline solution.

3.2. Potentio-dynamic polarization behavior of Zn anode with various additives

To clarify the effect of additives on H_2 evolution behavior, it is observed that the polarization behavior of each Zn-based gel anode using three electrode's cell to evaluate the overpotential for spontaneous H_2 evolution reaction. Fig. 3 shows the bi-directional potentio-dynamic polarization curves of Zn-based gel anode in 9 M KOH electrolyte. The electrochemical parameters (corrosion potential, corrosion current density) derived from Fig. 3 are summarized in Table 1. Generally, the modern theory of metallic

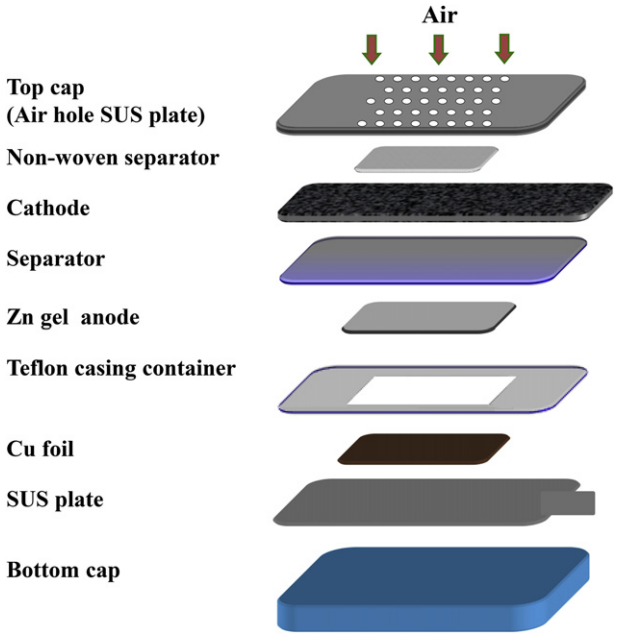

Fig. 1. Assembly diagram and component images of unit type Zn–air battery for evaluation.

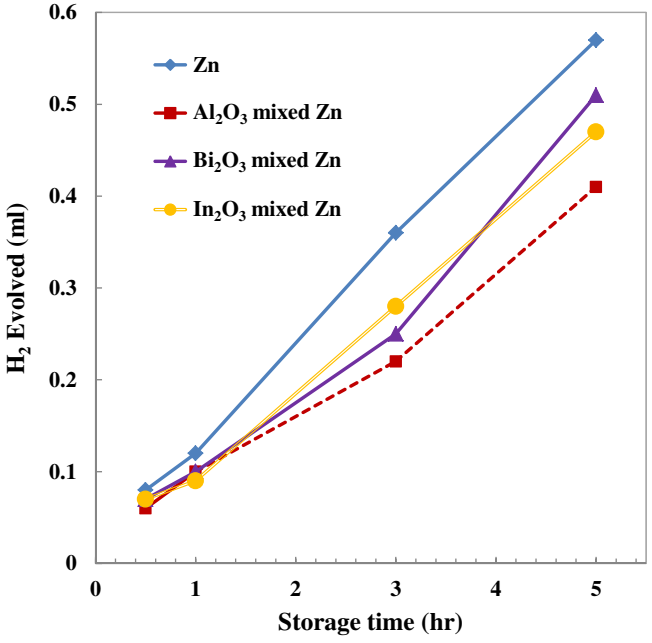

Fig. 2. Volumetric measurement of hydrogen spontaneously evolved on the surface of Zn gel anode at 60 °C.

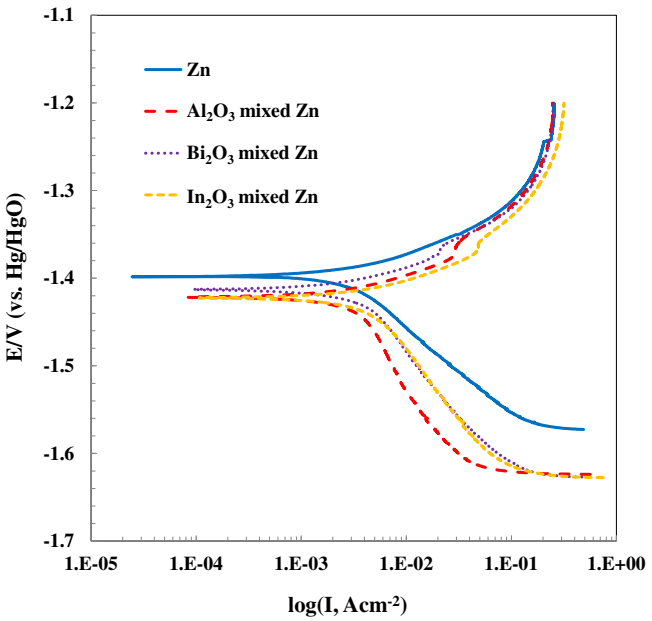

Fig. 3. potentio-dynamic polarization curves of Zn gel anodes with various additives in 9 M KOH electrolyte at a scan rate of 20 mV s^{-1} at room temperature.

corrosion in aqueous electrolyte is based on electrode kinetics. For the corrosion system consisted of a cathodic reaction and an anodic reaction, the application of the Butler–Volmer equation [27,28] and the mixed potential theory [29] results in the basic kinetic equation:

$$i = i_{\mathrm{corr}}\left\{\exp\left[\frac{2.303(E-E_{\mathrm{corr}})}{b_{\mathrm{a}}}\right] - \exp\left[-\frac{2.303(E-E_{\mathrm{corr}})}{b_{\mathrm{c}}}\right]\right\} \quad (1)$$

where E is the scanned potential applied to polarize the corrosion system; i is the external current density to the corresponding overpotential; E_{corr} and i_{corr} are the corrosion potential and corrosion current density, respectively; b_{c} and b_{a} are the cathodic and anodic Tafel slope, respectively. When E is far away from E_{corr}, Eq. (1) obeys the Tafel law [30]:

$$E = a \pm b \log |i| \quad (2)$$

where a is a constant, b equals to b_{c} or b_{a}. Eq. (2) indicates that the logarithm of the external current density varies linearly with the potential at high overpotential. The corrosion current density can be determined by extrapolating the straight line of E vs log $|i|$ back to the corrosion potential. In Fig. 3, however, it can be seen that the polarization curves obtained at the initial stage of the potentio-dynamic scan do not show the linear behavior. This is caused by the strong disturbance of another kind of charging current [31]. Thus, for the polarization curves, the potential range of the cathodic and anodic branches was selected to perform the linear fitting. In all cases, the equations fit the experimental curves well, with $R^2 > 0.99$, which indicates that the polarization curves show good linearity in the selected potential range.

Table 1
Electrochemical parameters of Zn anodes modified with various additives derived from potentio-dynamic polarization curves in 9 M KOH electrolyte.

Zn anodes	Corrosion potential (E_{corr}: V vs. Hg/HgO)	Corrosion current density (I_{corr}: μA cm^{-2})
Pure Zn	−1.398	512.5
Al_2O_3 mixed Zn	−1.422	423.6
Bi_2O_3 mixed Zn	−1.413	477.8
In_2O_3 mixed Zn	−1.422	473.3
Al_2O_3 coated Zn	−1.431	91.4

The corrosion potential (E_{corr}) was slightly shifted to a negative potential and corrosion current density (I_{corr}) was decreased in case of applying metal oxide additives into Zn gel anode. To understand electrochemical effects on anodic behavior of various additives addition to the Zn electrode, it can be also seen that when the potential was scanned from E_{corr} to −1.2 V (vs. HgO/Hg), the additives have little influences on anodic behavior of Zn gel anode. On the other hand, the cathodic behavior of Zn gel anode, which is mainly related with hydrogen evolution reaction, has been much affected by additives while scanned from E_{corr} to −1.60 V (vs. Hg/HgO). For each metallic oxide added Zn gel anode, its overpotential at a fixed current density (e.g., 0.01 A cm^{-2}) was higher than that of a pure Zn gel anode as shown in Fig. 3. Considering E_{corr}, and I_{corr}, Al_2O_3 mixed Zn gel anode shows the most favorable characteristics among the others, which is in accordance with hydrogen evolution behavior and corrosion rate of Zn-based anode with various additives.

3.3. Phenomenological analyses on corroded Zn surface after storage

Based on corrosion reaction of Zn, the thickness of Zn oxide film in alkaline aqueous solution can be expected to increase in proportion to the amount of hydrogen gas as measured in above results. Thus, we conducted SEM and EDS analyses on Zn anode surface to identify the oxidation degree of Zn anode after storage for 5 h. The quantitative analysis on oxygen concentration in the sub-surface region (~several μm orders) was conducted by EDS for different Zn anodes after immersing in 9 M KOH electrolyte for 5 h. The oxygen concentration of pure Zn anode (~0.8 at.%) after storage considerably increased up to ~12.3 at.%, compared with that of as-prepared Zn anode. It also showed the higher value than that (3.8–9.0 at.%) of Zn anodes with additives (Fig. 4). From this result, it is confirmed that the surface oxidation of Zn anode can be considered as corrosion by-product, while accompanying H_2 evolution during storage. Eventually, since the surface oxidation of Zn means the loss of active material involved in electrochemical work, the degree of self-discharge can be evaluated by only measuring the amount of hydrogen evolved from Zn surface during storing in alkaline electrolyte.

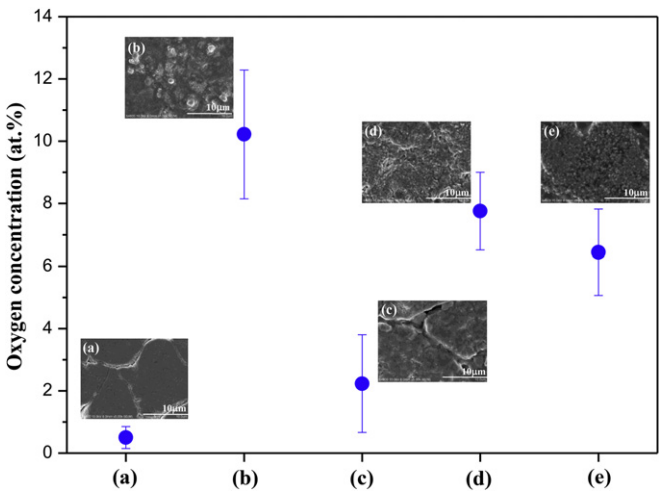

Fig. 4. SEM images and EDS analyses for (a) as-prepared Zn anode surface before immersion in 9 M KOH electrolyte, and Zn anode surface with (b) no additive, (c) Al_2O_3, (d) Bi_2O_3, (e) In_2O_3 additives after immersion in 9 M KOH electrolyte for 5 h.

3.4. Synthesis of Al-oxide coated Zn powder

In general, it is well understood that the surface modification is required to prevent from exposing to corrosive media by coating inert material. Therefore, we tried to modify Zn surface by Al_2O_3 coating layer among additives to retard H_2 evolution reaction rate. As described in experimental details, we have pure Zn powder chosen as a starting material, which was compared with the performances of modified Zn anode. The Al-oxide coated Zn was prepared by chemical solution process using Al-isopropoxide as an Al precursor. In order to determine proper temperature for heat treatment of hydrolyzed Al-isopropoxide dispersed Zn, we had thermal analysis (TGA-DSC) during heating at a scan rate of 10 °C min^{-1}. under Ar atmosphere. The TG and DSC of the gel were carried out at a heating rate of 10 °C min^{-1} up to 800 °C, in Ar atmosphere (Fig. 5A). DSC analysis was used to identify the solvent evaporation steps in the temperature range of 25–400 °C. In the temperature range from 25 °C to 300 °C, the DSC curve shows two endothermic peaks at 142.5 °C and 295.7 °C corresponding to the volatilization of absorbed water on the grain surface, isopropanol and solvent component, respectively. The second major weight loss that occurs in the temperature range from 250 °C to 350 °C is due to the pyrolysis of the organic groups (exothermic peak). Therefore, the decomposition of organic material in Al-isopropoxide was expected to be almost finished at 400 °C. It is believed that the thermal energy of 400 °C is considered to be enough to decompose Al-isopropoxide, resulting in Al-oxide layer on the Zn surface. Therefore, the heat treatment temperature was chosen to be 400 °C, considering low melting temperature (~420 °C) of pure Zn. The XRD analysis was conducted to clarify the crystal structure of Al compound produced by heat treatment at 400 °C. The XRD patterns are in good agreement with the standard data for the pure phase of Al_2O_3 with low crystallinity prepared by hydrolyzing aluminum alkoxides, as shown in Fig. 5B.

3.5. Phenomenological characterization of Al-oxide coated Zn powder

To identify the uniformity of Al_2O_3 coating on Zn powder, we carried out the EDS mapping on constituting elements of Al_2O_3 coated Zn powder. We could observe that the sub-micron sized Al_2O_3 particles were uniformly coated on Zn surface by Al EDS mapping analysis (Fig. 6A). To further clarify the chemical state of Al-based compound, the XPS analysis was performed and the results are presented in Fig. 6B. The Al2*p* (75.6 eV) could be confirmed to be Al_2O_3, which might be assigned by mixed polymorph forms of Al_2O_3 [32]. Additionally, the O1*s* peaks could be separated by two peaks (530.3 eV, and 531.9 eV), which can be assigned to be Al–O, Al–OH and Zn–O, referring to XPS analysis data on both types of synthetic Al-oxide and native Zn oxide. Especially, the duplicate assigns for Al–OH and Zn–O chemical bindings could be considered for O1s peak (531.9 eV). Consequently, based on the above results, we could identify the synthetic Al_2O_3 coating layer to be formed on the Zn anode surface by modification using Al-isopropoxide via chemical solution process and heat treatment.

3.6. Electrochemical characterization of Al-oxide coated Zn powder

In general, the demand on suppressing hydrogen evolution is crucial for both primary and secondary Zn–air batteries. The rate of hydrogen evolution reaction (HER) mainly depends on the overpotential of corresponding reaction on Zn anode surface. To evaluate the effect of surface modification on electrochemical performances of Zn anode, first of all, we compared the potentiodynamic polarization behaviors between pure Zn, Al_2O_3 mixed Zn, and Al_2O_3 coated Zn.

We identified that the E_{corr} was significantly shift to lower potential, and I_{corr} was much decreased by Al_2O_3 coating on Zn, indicating higher overpotential for H_2 evolution reaction than that of bare Zn and Al_2O_3 mixed Zn, as shown in Fig. 7A and Table 1. Thus, it is believed that the surface coating can be more effective way to suppress the H_2 evolution reaction than just adding metallic oxide powder into electrode. In order to clarify the coating effect on HER, the hydrogen gas volume evolved from the as-prepared Al_2O_3 coated Zn particles were measured by a volumetric method. Fig. 7B shows the measurement results of hydrogen evolution volume during storage in 9 M KOH electrolyte at 60 °C. We could observe a significant difference in HER behavior between the bare and Al_2O_3 coated Zn anodes. It is evident that Zn corrosion was quite intensive without the use of any additive and the volume of hydrogen evolution was approximately two times higher than for the optimal

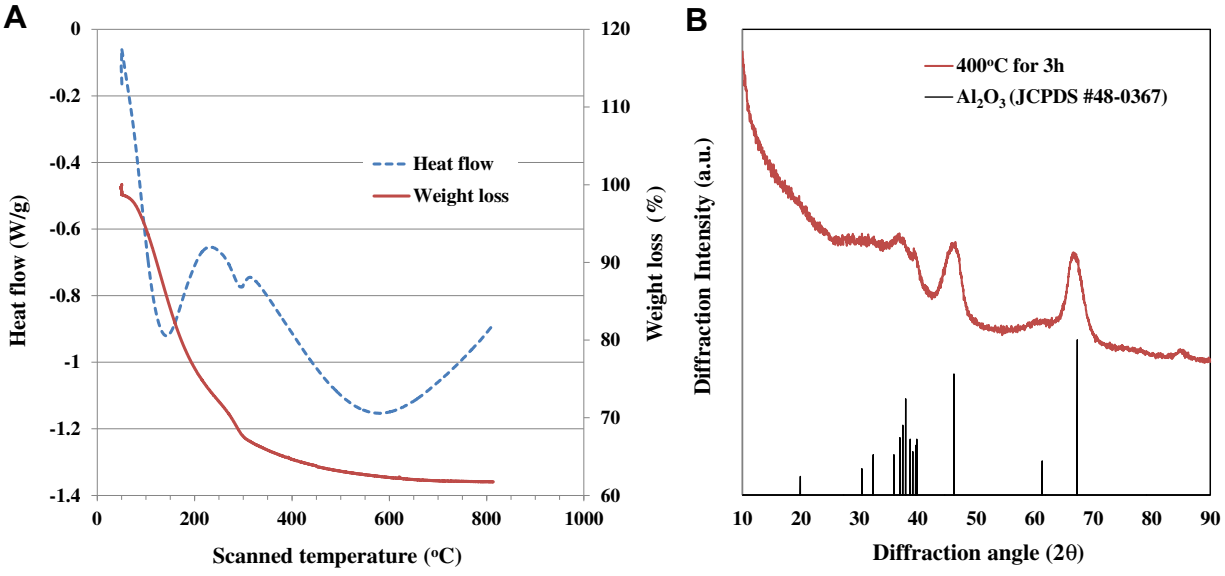

Fig. 5. (A) DSC and TG analyses for Al-isoporpoxide at a scan rate of 10°C min^{-1}. Under Ar atmosphere. (B) X-ray diffraction pattern of heat treated Al-isoporopoxide at 400 °C for 3 h under Ar atmosphere.

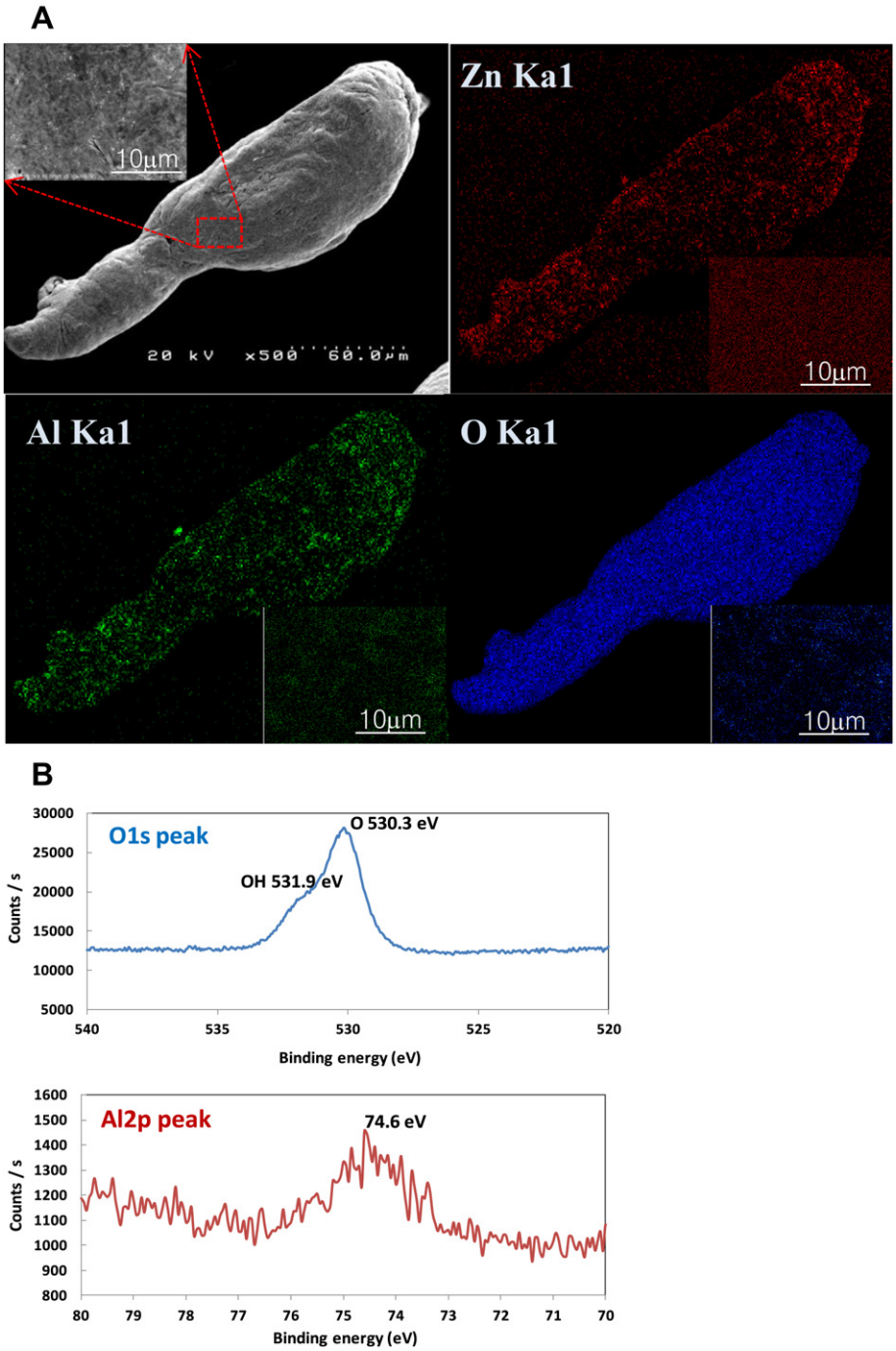

Fig. 6. (A) SEM and Al, Zn, and O energy dispersive spectrascopy (EDS) mapping images for Al_2O_3 coated Zn particle. (B) XPS spetra (Al2*p*, O1*s*) on the surface of Al_2O_3 coated Zn particle.

coating composition of 0.25 wt.% Al_2O_3 coated Zn powders. The remarkable effect of suppressing HER by Al_2O_3 coating on Zn powders was due to the fact that the surface of the Zn particles was protected by the Al_2O_3 layer which provided a passivation layer to prevent direct contact of Zn with the electrolyte.

3.7. Evaluation of Zn–air unit cell applying Al-oxide coated Zn powder

Furthermore, to examine the practical effect on cell performances by applying the Al_2O_3 coated Zn, we fabricated the unit cell applying the bare Zn, commercialized Zn alloy, and Al_2O_3 coated Zn as Zn gel anodes, and carbon supported electrode as an air cathode, as described in Fig. 1. We have chosen the commercialized Zn alloy (Zn–Bi(100 ppm)–In(200 ppm)–Al(65 ppm)), which has been designed for suppressing H_2 evolution, as an anode material of Zn–air battery for miniature hearing aids. The energy density of Zn–air rechargeable battery mainly depends on utilization efficiency of Zn anode material in alkaline electrolyte. The Zn fuel in anode cannot be fully utilized by oxidation of metallic Zn, while spontaneously evolving hydrogen gas on Zn surface in basic alkaline solution. To increase the discharge efficiency of Zn anode, the spontaneous self-discharge of Zn anode should be retarded to be as low as possible.

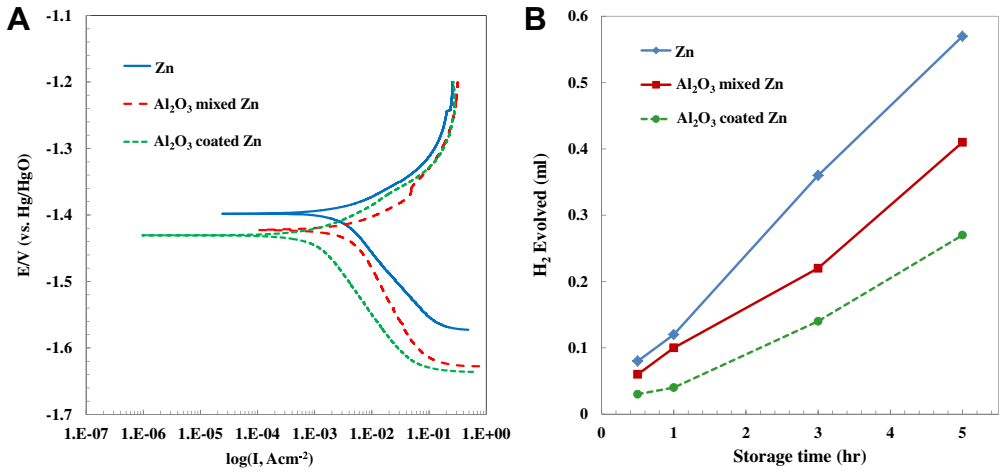

Fig. 7. (A) Comparison of volumetric amount of hydrogen spontaneously evolved on the surface of bare Zn, Al_2O_3 mixed Zn, and Al_2O_3 coated Zn gel anodes at 60 °C. (B) Comparison of potentio-dynamic polarization curves of bare Zn, Al_2O_3 mixed Zn and Al_2O_3 coated Zn anode in 9 M KOH electrolyte at a scan rate of 20 mV s^{-1} at room temperature.

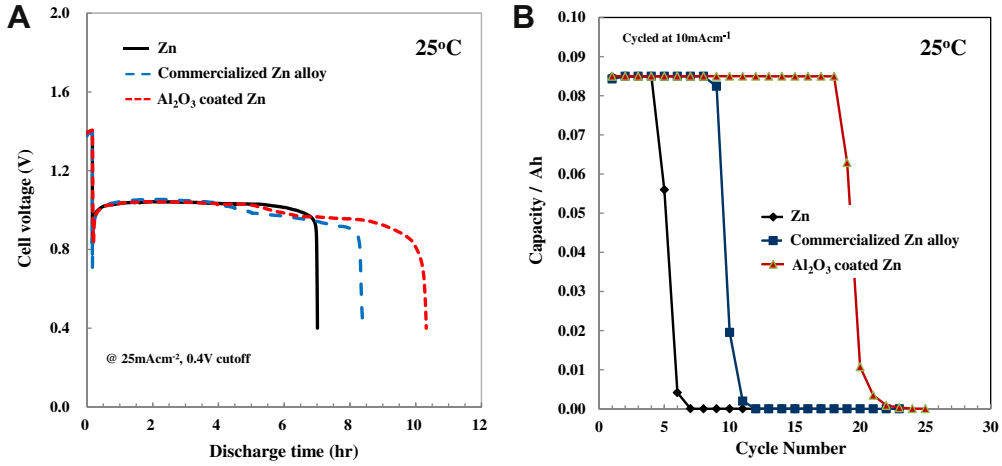

Fig. 8. (A) Comparison of discharge curves among bare Zn, commercialized Zn alloy, and Al_2O_3 coated Zn anode in 9 M KOH electrolyte at room temperature. (B) Comparison of cyclic durability among bare Zn, commercialized Zn alloy, and Al_2O_3 coated Zn anodes during electrochemical cycling in 9 M KOH electrolyte at room temperature.

We can measure the utilization efficiency of active material in Zn anode when the unit cell is discharged at a constant current of 25 mA cm^{-2}. As shown in Fig. 8A, the Al_2O_3 coated Zn showed the longer discharge time than pure Zn and commercialized Zn alloy anodes, which means the improved sustainability of Zn anode due to suppression of H_2 evolution. It is well explained that the control of spontaneous H_2 evolution is closely related with Zn oxidation, resulting in being inactive material for electrochemical discharge. Moreover, the electrical chargeability of different Zn anodes was measured at a current density of 10 mA cm^{-1}under with limited capacity cut-off condition. Similarly, the discharge capacity of bare Zn and commercialized Zn alloy anodes abruptly goes down to almost zero capacity at much earlier cycle number as shown in Fig. 8B. On the contrary, it is observed that the discharge capacity of Al_2O_3 coated Zn anode is maintained during longer cycle. Many reasons for cyclic degradation of Zn anode during electrochemical cycling have been suggested. In particular, the dendrite growth of Zn anodes resulting from the high solubility of Zn-based discharge products in the alkaline electrolyte was one of the main reasons responsible for the short cycle life. One effective way to solve this problem was to suppress the solubility of Zn-based discharge product by forming passivation layer on the Zn surface [26]. The improved cyclic behavior of Al_2O_3 coated Zn anode might be interpreted by above similar reasons. Therefore, based on various characterization of surface modified Zn anode material, it can be confirmed that the Al_2O_3 coated Zn is very potential as mercury-free anode material of next generation Zn–air battery for transportation and energy storage.

4. Conclusion

Metallic oxides have been also found to suppress the hydrogen evolution of Zn anode during storage in alkaline electrolyte, comparable to metal additives suggested up to now. Aluminum oxide has most effective ability against self-discharge spontaneously occurred under air atmosphere among various additives studied in this work. To further pronounce the positive effect on H_2 evolution reaction, technical approach such as surface coating has been also extensively investigated. The enhanced discharge efficiency can be explained by the formation of a thin oxide coating layer on the surface of bare Zn particles that can prevent Zn from directly exposing to the KOH electrolyte and minimize the spontaneous side reactions such as hydrogen evolution within the batteries. Furthermore, the electrochemically cyclic behavior of the Zn anode has been also remarkably enhanced by Al_2O_3 coating on the Zn surface. Consequently, it can be suggested that the Al_2O_3

coated Zn is very promising as mercury-free anode material for Zn-air battery with higher energy density.

Acknowledgement

This work was supported by the Metal-Air Fuel Cell Development Program funded by the Agency for Defense Development (ADD, Korea).

References

[1] D. Linden, T.B. Reddy, in: Handbook of Batteries, third ed., McGraw-Hill, 2002 (Chapter 13).
[2] F.G. Will, in: Proceedings of 13th Annual Battery Conference on Applications and Advances, IEEE, Long Beach, CA, USA, 1998.
[3] D.P. Gregory, Metal-air Batteries, Mills & Boon Limited, London, 1972.
[4] C.L. Mantell, in: Batteries and Energy Systems, second ed., McGraw-Hill Publishing Company, New York, 1983.
[5] D. Linden, Handbook of Batteries, McGraw-Hill Publishing Company, New York, 1994.
[6] C.J. Lan, T.S. Chon, P.H. Lin, T.P. Perng, Journal of New Materials for Electrochemical Systems 9 (2006) 27.
[7] Energizer Zinc Air Primatic Handbook (2009).
[8] J.S. Lee, S.T. Kim, R. Cao, N.S. Choi, M. Liu, K.T. Lee, J. Cho, Advanced Energy Materials 1 (2011) 34.
[9] K. Kim, Y.H. Cho, S.W. Eom, H.S. Kim, J.H. Yeum, Materials Research Bulletin 103 (2010) 34.
[10] B. Beverskog, I. Puigdommenech, Corrosion Science 39 (1997) 107.
[11] C. Chakkaravarthy, A.K.A. Waheed, H.V.K. Udupa, Journal of Power Sources 6 (1981) 203.
[12] T.I. Devyatkina, Y.L. Gun'ko, M.G. Mikhalenko, Russian Journal of Applied Chemistry 74 (2001) 1122.
[13] L.F. Urry, US Patent 6,022,639 (1996).
[14] J. Dobryszycki, S. Biallozor, Corrosion Science 43 (2001) 1309.
[15] C.W. Lee, K. Sathiyaanarayanan, S.W. Eom, M.S. Yun, Journal of Power Sources 160 (2006) 1436.
[16] Y. Ein-Eli, M. Auinat, D. Straosvetsky, Journal of Power Sources 114 (2003) 330.
[17] C.W. Lee, K. Sathiyaanarayanan, S.W. Eom, M.S. Yun, Journal of Power Sources 159 (2006) 1474.
[18] C. Zhang, J.M. Wang, L. Zhang, J.Q. Zhang, C.N. Cao, Journal of Applied Electrochemistry 31 (2001) 1049.
[19] R. Shivkumar, G.P. Kalaignan, T. Vasudevan, Journal of Power Sources 75 (1998) 90.
[20] G. Coates, N.A. Hampson, A. Marshall, D.F. Porter, Journal of Applied Electrochemistry 4 (1974) 75.
[21] R. Othman, W.J. Basirun, A.H. Yahaya, A.K. Arof, Journal of Power Sources 103 (2001) 34.
[22] X. Zhu, H. .Yang, Y. Cao, X. Ai, Electrochimica Acta 49 (2004) 2533.
[23] T.G. COMPANY, World Patent WO01/890650 (2002).
[24] R.E.F. Einerhand, W.H.M. Visscher, E. Barendrecht, Journal of Applied Electrochemistry 18 (1988) 799.
[25] Y.D. Cho, G.T. Fey, Journal of Power Sources 184 (2008) 610.
[26] H. Yang, X. Meng, E. Yang, X. Wang, Z. Zhou, Journal of Electrochemical Society 151 (2004) A389.
[27] J.A.V. Butler, Transactions of the Faraday Society 19 (1924) 734.
[28] T. Erdey-Gruz, M. Volmer, Zeitschrift für Physikalische Chemie 150A (1930) 203.
[29] C. Wagner, W. Traud, Zeitschrift fur Elektrochemie 44 (1938) 391.
[30] J. Tafel, Zeitschrift für Physikalische Chemie 50 (1905) 641.
[31] X.L. Zhang, Zh.H. Jiang, Zh.P. Yao, Y. Song, Zh.D. Wu, Corrosion Science 51 (2009) 581.
[32] J.T. Kloprogge, L.V. Duong, B.J. Wood, R.L. Frost, Journal of Colloid and Interface Science 296 (2000) 572.